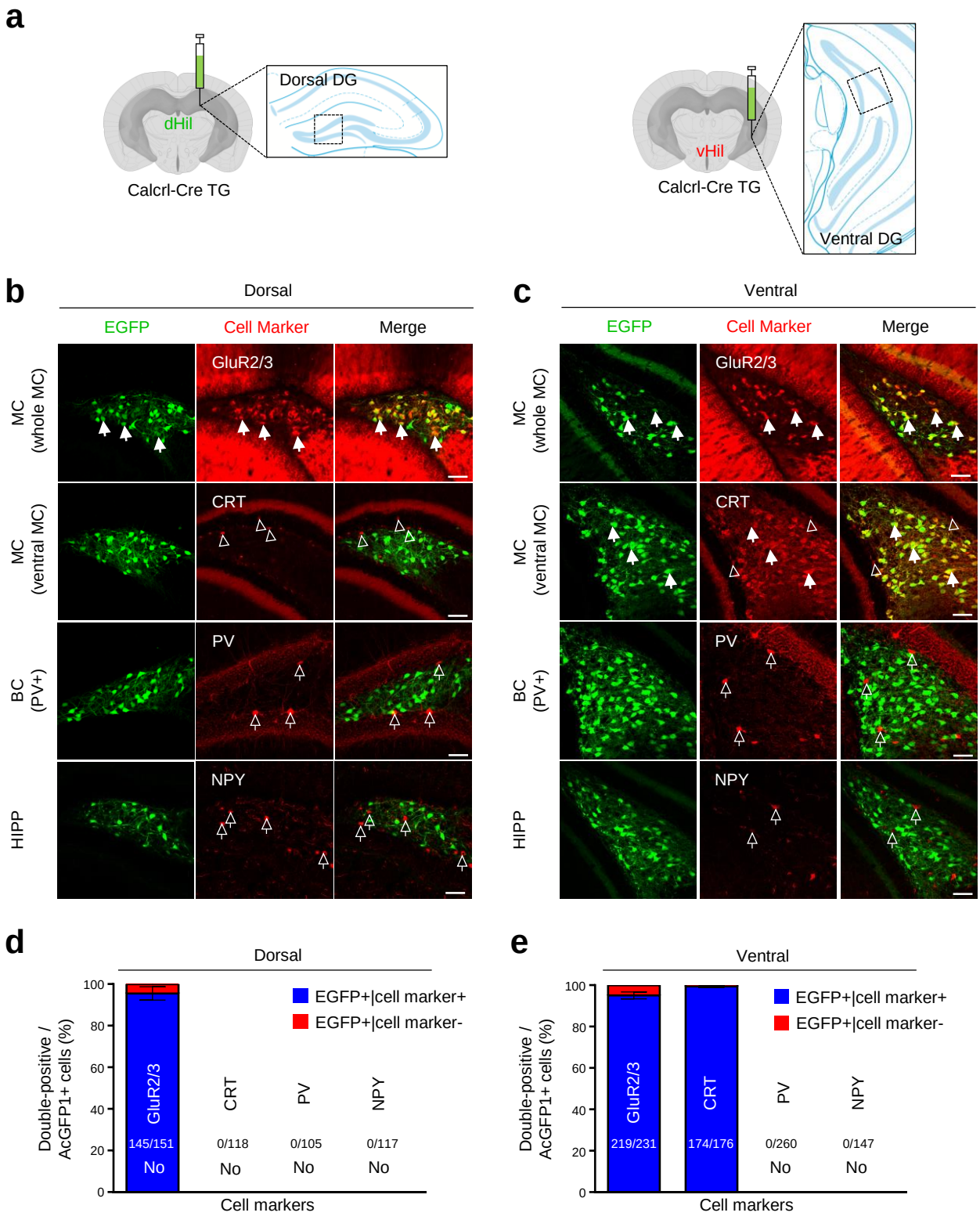
a
dHil
Dorsal DG
Calcrl-Cre TG
vHil
Calcrl-Cre TG
Ventral DG
b
Dorsal
EGFP
Cell Marker
Merge
MC (whole MC)
GluR2/3
MC (ventral MC)
CRT
BC (PV+)
PV
HIPP
NPY
c
Ventral
EGFP
Cell Marker
Merge
MC (whole MC)
GluR2/3
MC (ventral MC)
CRT
BC (PV+)
PV
HIPP
NPY
d
Dorsal
Double-positive / AcGFP1+ cells (%)
EGFP+|cell marker+
EGFP+|cell marker-
GluR2/3
145/151
No
CRT
0/118
No
PV
0/105
No
NPY
0/117
No
Cell markers
e
Ventral
Double-positive / AcGFP1+ cells (%)
EGFP+|cell marker+
EGFP+|cell marker-
GluR2/3
219/231
CRT
174/176
PV
0/260
No
NPY
0/147
No
Cell markers

Supplementary Fig. 1 Calcrl-Cre mice displays a high levels of specificity of MCs (Related to Fig. 1) a Calcrl-Cre mice were unilaterally injected Cre-dependent EGFP expressing virus into either dHil or vHil, respectively **b, c** Representative coronal images showing of MC specific fluorescence labeling in dHil (b) and vHil (c) of Calcrl-Cre mice. EGFP expressing cells were immunostained for GluR2/3 (GluR2/3; Pan MCs marker), Calretinin (CRT, vMCs marker), parvalbumin (PV; subpopulation of basket cell marker), neuropeptide Y (NPY, hilar perforant path-associated cell marker). Solid arrow heads bar: representative doubly labeled cells. Open arrow heads bar: cells labeled only with markers. Open arrow heads: calretinin-positive interneurons. Scale bar, 50 μm. **d, e** The quantitative analysis of MCs specificity of Calcrl-Cre mice. Labeled cells in dHil (d) were highly colocalized with GluR2/3 (95%±1.4), but not colocalized with other marker (CRT, PV, and NPY). Labeled cells in vHil (e) were colocalized with both GluR2/3 (95%±1.7) and CRT (99%±0.6), their cells were no colocalized with marker (PV and NPY). (n = 3, mice per group). All data represented as mean ± SEM.

a

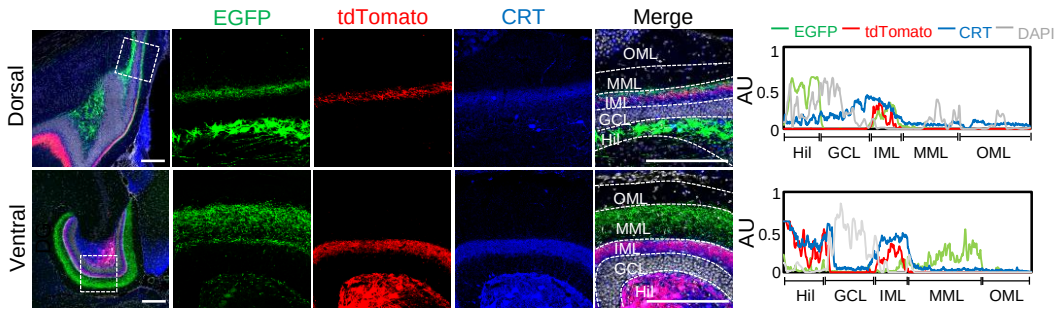

Supplementary Fig. 2 Axonal fibers in MML of vDG are originated from dMCs (Related to Fig. 1) a Representative fluorescence images with calretinin (CRT) immunostaining of the dorsal (top) and ventral (bottom) DG from Fig. 1A. Hil, hilus; GCL, granule cell layer; IML, inner molecular layer; MML, middle molecular layer; OML, outer molecular layer. Scale bar, 200 μm.

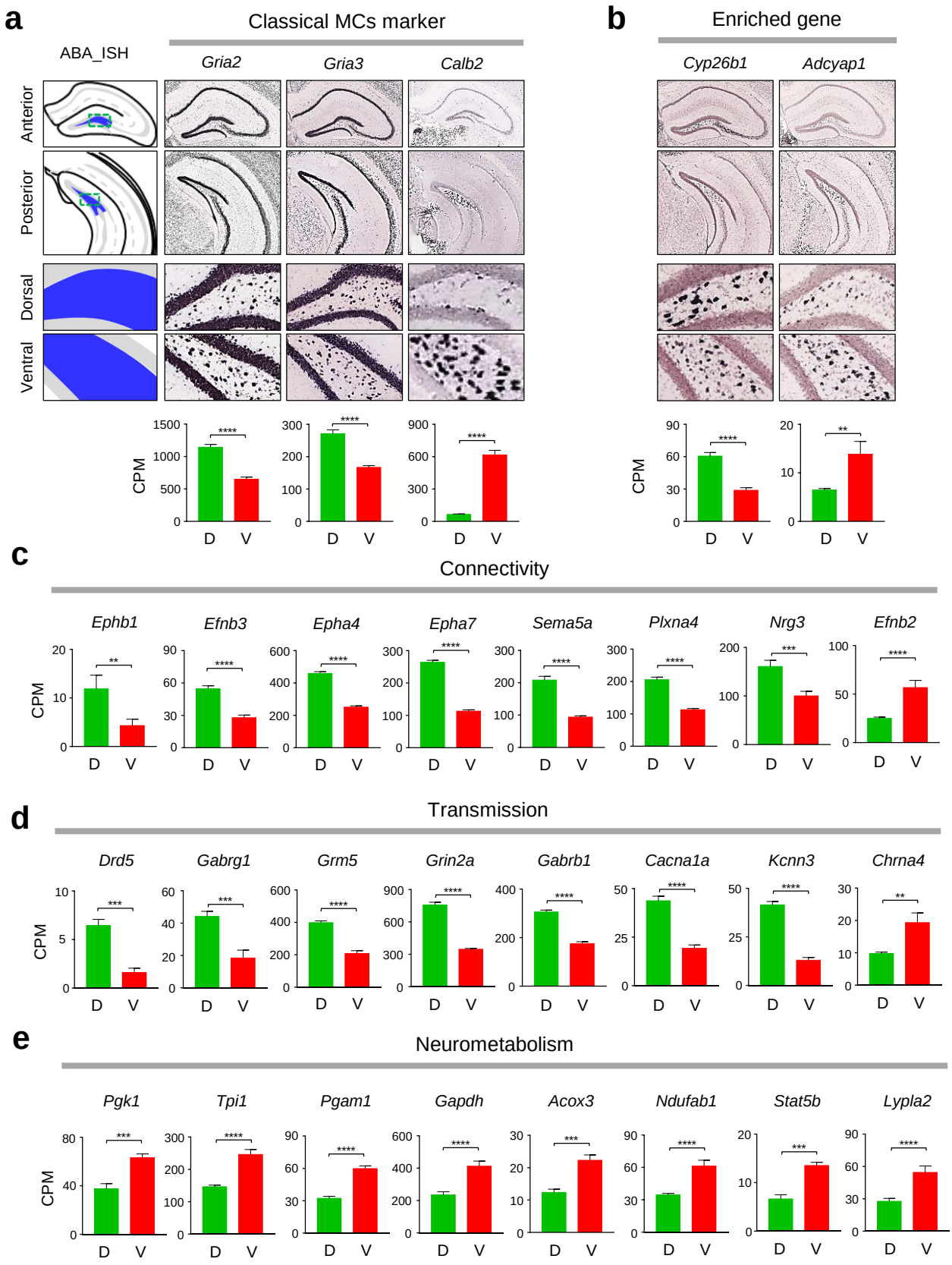
a
Classical MCs marker
ABA_ISH
Gria2
Gria3
Calb2
Anterior
Posterior
Dorsal
Ventral
CPM
D
V
b
Enriched gene
Cyp26b1
Adcyap1
c
Connectivity
Ephb1
Efnb3
Epha4
Epha7
Sema5a
Plxna4
Nrg3
Efnb2
d
Transmission
Drd5
Gabrg1
Grm5
Grin2a
Gabrb1
Cacna1a
Kcnn3
Chrna4
e
Neurometabolism
Pgk1
Tpi1
Pgam1
Gapdh
Acox3
Ndufab1
Stat5b
Lypla2

Supplementary Fig. 3 dMCs and vMCs express differential subsets of genes associated with various functions (Related to Fig. 3) a Representative ISH images from ABA showing distribution of MCs marker (Gria2 and Gria3; MCs marker, Calb2; vMCs marker) along the DV axis of the DG. **b** Representative ISH images from ABA showing differential enriched genes pattern (Cyp26b1; dMCs-, Adycap1; vMCs-enriched) along the DV of the DG. **c-e** Representative gene expression patterns in differential enrichment of MC subpopulations associated with connectivity (c), transmission (d), and neurometabolism (e) categories. **p < 0.01, ***p < 0.001, and ****p < 0.0001, quasi-likelihood test. All data represented as mean ± SEM.

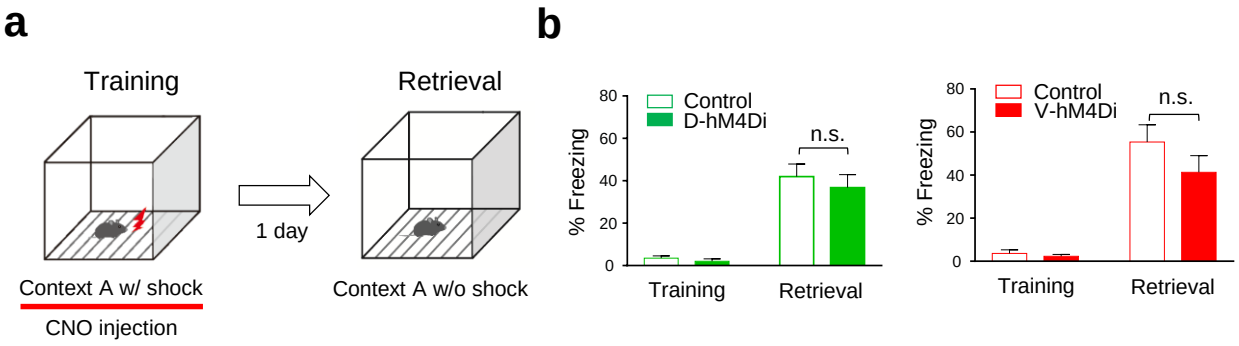

Supplementary Fig. 4 Contextual fear memory acquisition is not interfered by MC inhibition along the DV axis (Related to Fig. 5) a Experimental procedure for contextual fear conditioning. **b** Effect of chemogenetic inhibition of either dMCs or vMCs on freezing levels. For dMCs group; DREADD ($F_{1,18}$=0.5022, p=0.4876); encoding ($F_{1,18}$=81,17, p<0.0001); interaction ($F_{1,18}$=0.2066, p=0.6549). For vMCs groups; DREADD ($F_{1,19}$=1.703, p=0.2075); encoding ($F_{1,19}$=72,4, p<0.0001); interaction ($F_{1,19}$=1.42, p=0.2480). Two-way repeated-measure ANOVA, Bonferroni post test. All data represented as mean ± SEM.

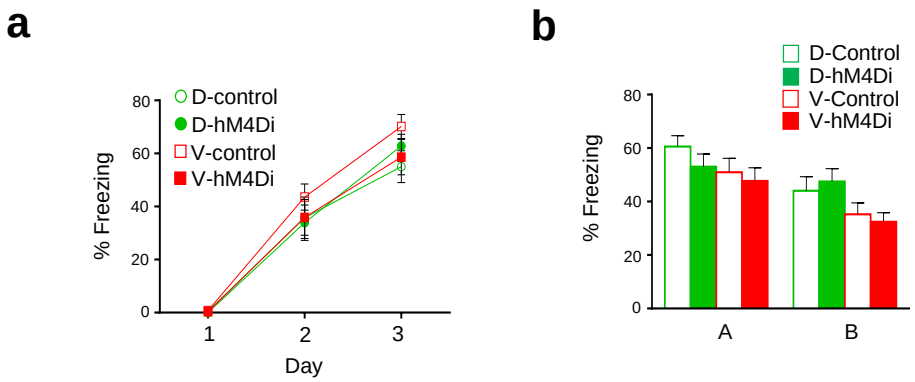

Supplementary Fig. 5 Contextual fear learning and generalization is consistent within all comparison groups (Related to Fig. 5) a Freezing level in context A during acquisition. The mice trained in context A through 3 days. Comparison groups; $F_{3,33}$=1.008, p=0.4017; learning; $F_{2,66}$=204, p<0.0001; interaction: $F_{3,33}$=0.7028, p=0.6483; Two-way repeated-measure ANOVA. **b** Contextual generalization in context B. the mice were exposed alternatively in between context A and B. Comparison groups; $F_{3,70}$=2.652, p=0.0554; day; $F_{1,70}$=19.81, p<0.0001; interaction: $F_{3,70}$=0.6876, p=0.5626; Two-way repeated-measure ANOVA. All data represented as mean ± SEM.

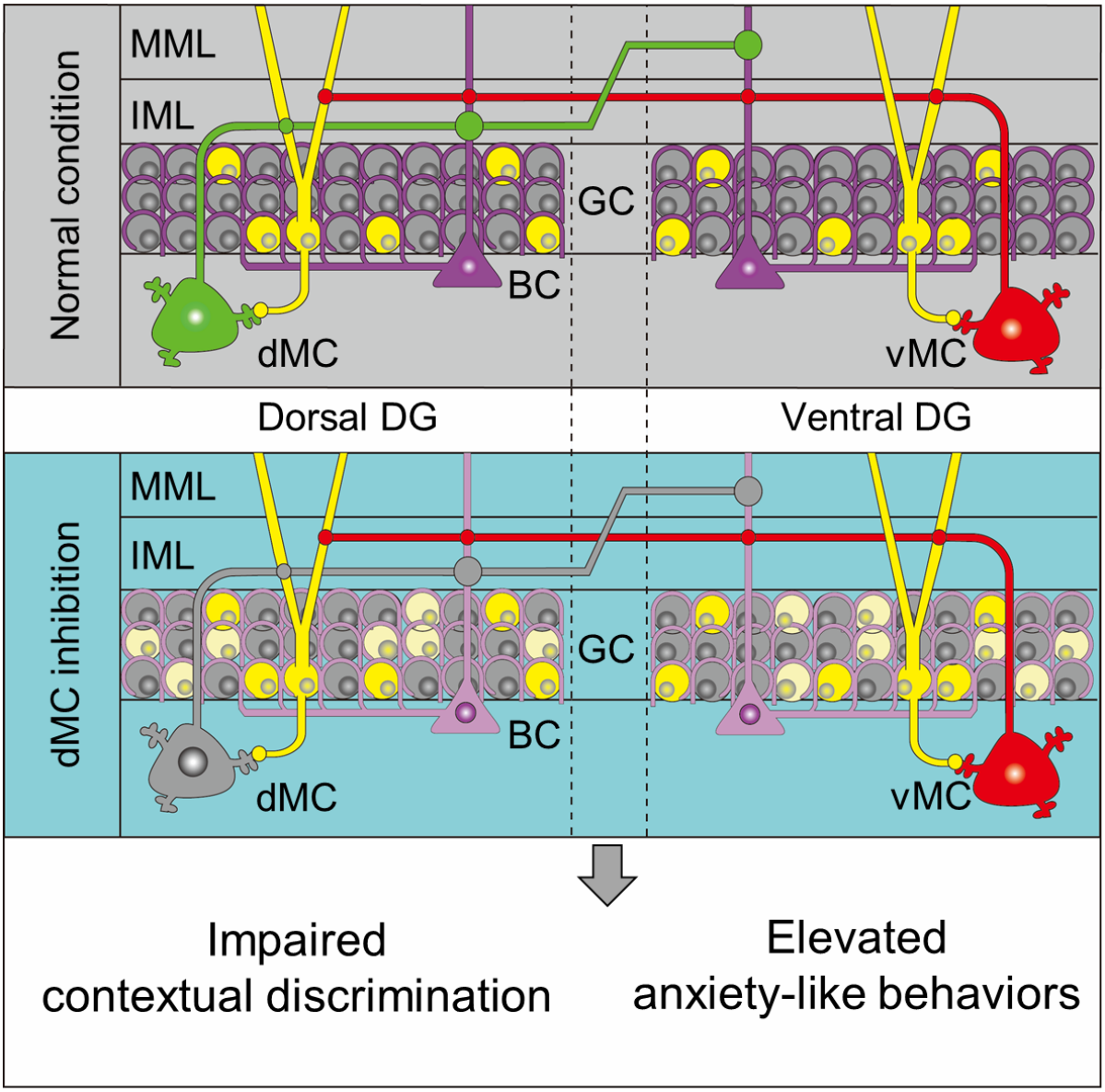

Supplementary Fig. 6 Schematic illustration of dorsoventral heterogeneity of MCs. dMCs and vMCs extend distinct axonal projection along DV axis of DG. Long-range axonal projection of dMCs, but not vMCs, provide net inhibitory control of GCs across the longitudinal axis of the DG, possibly through PV+BCs. Inhibition of dMCs increases behavioral anxiety and disables rapid contextual discrimination.

Supplementary Table 3

Fig	Sample size (n)	Type of statistical analysis	Values
Fig. 1d	Axonal fiber of dMCs and vMCs: n = 3, 3 slices per mice	Two-way mseausres ANOVA	Molecular layers (dMC) F (1, 48) = 7.913, P = 0.0071 DV axis (dMC) F (2, 48) = 53.94, P < 0.0001 Interaction (dMC) F (2, 48) = 83.78, P < 0.0001 Molecular layers (vMC) F (1, 48) = 391.6, P < 0.0001 DV axis (vMC) F (2, 48) = 26.87, P < 0.0001 Interaction (vMC) F (2, 48) = 15.74, P < 0.0001
Fig. 1f	Axonal fiber of dMCs and vMCs: n = 3, 3 slices per mice	Two-way mseausres ANOVA	Molecular layers (dMC) F (1, 48) = 40.24, P < 0.0001 DV axis (dMC) F (2, 48) = 97.12, P < 0.0001 Interaction (dMC) F (2, 48) = 79.2, P < 0.0001 Molecular layers (vMC) F (1, 48) = 77.02, P < 0.0001 DV axis (vMC) F (2, 48) = 24.29, P < 0.0001 Interaction (vMC) F (2, 48) = 22.14, P < 0.0001
Fig. 2e	MC proportions: n = 5	Paired t test	T (4) = 5.398; P = 0.0057
Fig. 3c	Expression of gria3, dMCs, n = 3; vMCs, n = 3	Unpaired t test	T (4) = 1.374; P = 0.2414
	Expression of calb2, dMCs, n = 3; vMCs, n = 3	Unpaired t test	T (4) = 12.46; P = 0.0002
Fig. 4c	Induction of DV of MCs c-fos: Naïve, n = 5; CFC, n = 6	Unpaired t test	T (31) = 8.212; P < 0.0001
Fig. 4h	Acute inhibition of dMCs on dGCs activity: D- and V-control, n = 5; inhibition of dMCs, n = 5; 3 slices per mice	Unpaired t test	T (28) = 4.923; P < 0.0001
	Acute inhibition of dMCs on vGCs activity: D- and V-control, n = 5; inhibition of dMCs, n = 5; 3 slices per mice	Unpaired t test	T (28) = 4.835; P < 0.0001
Fig. 4i	Acute inihibition of vMCs on dGCs excitatbility: D- and V-control n=5; inhibition of vMCs n=3 each sections: 3 per mice	Unpaired t test	T (22) = 1.73; P = 0.0976
	Acute inihibition of vMCs on dGCs excitatbility: D- and V-control n=5; inhibition of vMCs n=3 each sections: 3 per mice	Unpaired t test	T (22) = 1.714; P = 0.1005
Fig. 4k	Acute inihibition of dMCs on dBCs excitatbility D-control n=3; Inhibition of dMCs n=5 each sections: 2 per mice	Unpaired t test	T (14) = 2.003; P = 0.0649
	Acute inihibition of dMCs on vBCs excitatbility: D-control n=3; Inhibition of dMCs n=5 each sections: 2 per mice	Unpaired t test	T (14) = 3.357; P = 0.0047
Fig. 4l	Acute inihibition of dMCs on dBCs number: D-control n=3; Inhibition of dMCs n=5 each sections: 2 per mice	Unpaired t test	T (14) = 1.32; P = 0.2080
	Acute inihibition of dMCs on vBCs number: D-control n=3; Inhibition of dMCs n=5 each sections: 2 per mice	Unpaired t test	T (14) = 0.8029; P = 0.4355
Fig. 5c	Acute inhibition of dMCs in EPM: D-control n=9; Inhibition of dMCs n=10	Unpaired t test	T (17) = 2.261; P = 0.0372
	Acute inhibition of vMCs in EPM: V-control n=9; Inhibition of dMCs n=10	Unpaired t test	T (17) = 1.288; P = 0.2149
Fig. 5d	Acute inhibition of dMCs in OFT: D-control n=9; Inhibition of dMCs n=10	Unpaired t test	T (17) = 4.566; P = 0.0003
	Acute inhibition of vMCs in OFT: V-control n=9; Inhibition of dMCs n=10	Unpaired t test	T (17) = 0.4139; P = 0.6841
Fig. 5g	D-control on discrimination training: n=10	Two-way repeated-measures ANOVA Bonferroni post test	Block: F (5, 95) = 5.563; P = 0.0002 Context: F (1, 19) = 39.43; P < 0.0001 Interaction: F (5, 95) = 2.619; P = 0.0290
	D-hM4Di on discrimination training: dMCs n=8	Two-way repeated-measures ANOVA Bonferroni post test	Block: F (5, 75) = 6.699; P < 0.0001 Context: F (1, 15) = 35.49; P < 0.0001 Interaction: F (5, 150) = 1.966; P = 0.0935
Fig. 5h	V-control on discrimination training: n=10	Two-way repeated-measures ANOVA Bonferroni post test	Block: F (5, 95) = 1.681; P = 0.1467 Context: F (1, 19) = 68.5; P < 0.0001 Interaction: F (5, 95) = 16.41; P < 0.0001
	V-hM4Di on discrimination training: n=9	Two-way repeated-measures ANOVA Bonferroni post test	Block: F (5,85) = 3.627; P = 0.0051 Context: F (1, 17) = 43; P < 0.0001 Interaction: F (5, 85) = 6.224; P < 0.0001
Fig. 5i	Discrimination training of dMC group on block 2-3: D-control, n=10; inhibition of dMCs, n=8	Two-way repeated-measures ANOVA Bonferroni post test	Context: F (1, 34) = 23.89; P < 0.0001 DREADD: F (1, 34) = 0.6758; P = 0.4167 Interaction: F (1, 34) =4.139; P = 0.0498
	Discrimination training of dMC group on block 5: D-control, n=10; inhibition of dMCs, n=8	Two-way repeated-measures ANOVA Bonferroni post test	Context: F (1, 34) = 45.73; P < 0.0001 DREADD: F (1, 34) = 0.05068; P = 0.8232 Interaction: F (1, 34) =0.0125; P = 0.9116

Fig. 5j	Discrimination training of vMC group on block 2-3: V-control, n=10; inhibition of vMCs, n=9	Two-way repeated-measures ANOVA Bonferroni post test	Context: F (1, 36) = 87.51; P = 0.0173 DREADD: F (1, 36) = 0.7124; P = 0.4042 Interaction: F (1, 36) =1.973; P = 0.1687
	Discrimination training of vMC group on block 5: V-control, n=10; inhibition of vMCs, n=9	Two-way repeated-measures ANOVA Bonferroni post test	Context: F (1, 36) = 90.04; P < 0.0001 DREADD: F (1, 36) = 2.237; P = 0.6855 Interaction: F (1, 36) = 3.321; P = 0.0767
Supplementary Fig. 4b	Contextual fear memory encoding of dMC group: D-control, n=9; D-hM4Di, n=11	Two-way repeated-measures ANOVA	Encoding: F (1, 18) = 81.17; P < 0.0001 DREADD: F (1, 18) = 0.5022; P = 0.4876 Interaction: F (1, 18) = 0.2066; P = 0.6549
	Contextual fear memory encoding of vMC group: D-control, n=10; D-hM4Di, n=11	Two-way repeated-measures ANOVA	Encoding: F (1, 19) = 72.4; P < 0.0001 DREADD: F (1, 19) = 1.703; P = 0.2075 Interaction: F (1, 19) = 1.42; P = 0.2480
Supplementary Fig. 5a	Contextual fear leaning D-control, n=10; D-hM4Di, n=8 V-control, n=10; V-hM4Di, n=9	Two-way repeated-measures ANOVA	Comparison groups: F (3, 33) =1.008; P < 0.4017 Learning: F (2, 66) = 204; P < 0.0001 Interaction: F (3, 33) = 0.7028; P = 0.6483
Supplementary Fig. 5b	Generalization test: D-control, n=10; D-hM4Di, n=8 V-control, n=10; V-hM4Di, n=9	Two-way repeated-measures ANOVA	Comparison groups: F (3, 70) =2.652; P = 0.0554 Contexts: F (1, 70) = 19.81; P < 0.0001 Interaction: F (3, 70) = 0.6876; p = 0.5626

Supplementary Movie 1 (Related to Fig. 1h): Three-dimensional imaging of dMCs and vMCs projections

The movie shows three-dimensional axonal projection of dMCs (green) and vMCs (red) in the intact hippocampus. Calcrl Cre mice were injected bilaterally with Cre-dependent expressing EGFP and tdTomato virus into dHil and vHil, respectively (Fig. 1). The brain was imaged through whole brain, and individual sectioned images were reconstructed into whole structure of hippocampus.

Supplementary Table 1 (Related to Fig. 3d): List of DEGs of dMCs and vMCs

Supplementary Table 2 (Related to Fig. 3j, k): List of functionally categorized DEGs of dMCs and vMCs

Supplementary Table 3: Statistical analysis